PHYSICAL REVIEW E **81**, 020403(R) (2010)

Effective interactions and melting of a one-dimensional defect lattice within a two-dimensional confined colloidal solid

Yu-Hang Chui,[1] Surajit Sengupta,[2,3] Ian K. Snook,[4] and Kurt Binder[1]

[1]*Institut für Physik, Johannes-Gutenberg Universtät, Staudinger Weg 7, D-55099 Mainz, Germany*

[2]*Centre for Advanced Materials, Indian Association for the Cultivation of Science, 2A and 2B Raja S.C. Mallik Road, Jadavpur, Kolkata 700 032, India*

[3]*Advanced Materials Research Unit, Satyendra Nath Bose National Centre for Basic Sciences, Block-JD, Sector-III, Salt Lake, Kolkata 700 098, India*

[4]*Applied Physics, School of Applied Science, RMIT University, P.O. Box 2476V, 3001 Melbourne, Australia*

(Received 24 November 2009; revised manuscript received 9 January 2010; published 22 February 2010)

We report Monte Carlo studies of a two-dimensional soft colloidal crystal confined in a strip geometry by parallel walls. The wall-particle interaction has corrugations along the length of the strip. Compressing the crystal by decreasing the distance between the walls induces a structural transition characterized by the sudden appearance of a one-dimensional array of extended defects each of which span several lattice parameters, a "soliton staircase." We obtain the effective interaction between the solitons. A Lindemann criterion shows that the reduction in dimensionality causes the finite soliton lattice to readily melt as the temperature is raised.

DOI: 10.1103/PhysRevE.81.020403 PACS number(s): 82.70.Dd, 64.75.Xc

There are many examples of condensed-matter systems where extended defects in some order-parameter field behave as effective "particles" which themselves undergo order-disorder transitions with important consequences for the properties of the original system. One can easily recall many examples such as charge [1] or spin [2] density waves, vortex matter [3], Skyrmions [4] in fractional quantum Hall systems, and domain walls in commensurate-incommensurate phases [5]. In many of these examples, the typical size of these defects is much larger than the smallest relevant microscopic length scale. Investigation of the properties of such defect lattices requires knowledge of the effective interactions between defects which are usually difficult to measure directly in experiments. They are also difficult to obtain from computer simulations because of the large difference in length scales involved and can usually be computed only within a mean-field approach and in the highly dilute limit [6]. In this Rapid Communication we describe a simple example involving extended defects in a colloidal solid [7,8] where, on the other hand, such effective interactions may be obtained to great accuracy using a relatively small system with appropriate use of finite-size techniques.

In a recent work [9], we have shown that one can produce novel defect states in a colloidal crystal confined within a narrow quasi-one-dimensional strip [10] by deforming it in a suitable way. We perform constant number, N, volume, V, and temperature, T, Monte Carlo simulations [11] of a simple model solid with particles interacting with a potential [12–14] $V(r)=\varepsilon(\frac{\sigma}{r})^{12}$ at a distance r. The solid consisting of $N=n_y\times n_x$ unit cells with lattice parameter a is confined in a channel of length $L_y=n_y a$ and width $D=(n_x-\Delta)a\sqrt{3}/2$, where Δ is a "misfit" parameter [Fig. 1 (inset)]. Periodic-boundary conditions are assumed in the y direction whereas, in the x direction, the crystalline strip is confined by two fixed walls composed of two rows of immobile particles. When $\Delta=0$, one obtains a triangular crystalline solid between the walls at zero tensile stress σ. With increasing misfit Δ (i.e., tensile strain) σ increases up to some critical value, where a transition occurs that reduces n_x by one. At constant density, the n_y extra particles of the row that disappears are distributed equally among the n_x-3 inner rows of the strip [9] making the resulting average lattice spacing $a'=a(n_x-3)/(n_x-2)$ incommensurate with the effective periodic potential due to the rows of fixed particles. This leads to the formation of a "soliton staircase" [9] along the length of the walls, (accompanied by a pattern of standing strain

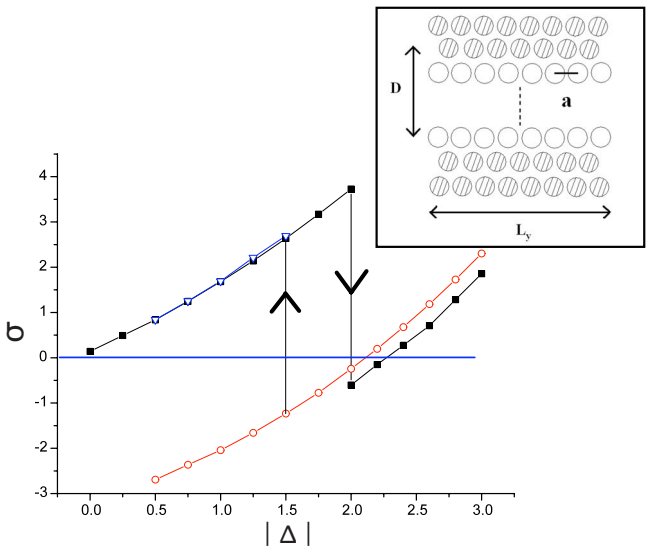

FIG. 1. (Color online) Internal stress $\sigma=\sigma_{xx}-\sigma_{yy}$ (in Lennard-Jones units) in the confined crystalline strip plotted vs Δ, for the case of a system started with $n_x=30$, $n_y=108$ (full symbols) and a system started with $n_x=29$, $n_y=108$ with the 108 extra particles distributed among the 27 inner rows, (open symbols). Curves are guides to the eye only. Inset: a schematic sketch of our geometry: we study a system of size D in x direction and L_y in the y direction, apply periodic boundary condition along the y axis, while the boundary in the x direction is created by two rows of fixed particles (shaded) on the ideal positions of a perfect triangular lattice at each side. In the fully commensurate case, $D=n_x a\sqrt{3}/2$.

waves in the crystal) according to the Frenkel-Kontorova mechanism [15]. The number of solitons produced is given by $n_s = n_y/(n_x - 3)$ [9] since each soliton contains a single excess particle per row. Here we extend our study and investigate the structural and mechanical properties of the system and show that the soliton superstructure in confined crystals behaves as a one-dimensional system of extended "particle"-like excitations which interact among themselves via an "effective" harmonic potential. We show how to extract the harmonic "spring constant" of this effective lattice and study the gradual melting of the soliton lattice into a soliton fluid caused by raising the temperature. We expect our calculations to be of direct relevance to experiments on confined colloidal crystals [7,8,16].

In order to extract properties of the defect system, we need to obtain the size and position of the individual defects. We describe below two independent techniques we use for this purpose which obtain near identical results lending added weight to our conclusions:

(1) *the ring method:* here, we identify the particles which belong to a single defect using the topologically defined concept of *shortest path* (SP) ring structures; the procedure is discussed at length in Refs. [17–19] to which we refer the interested reader for details. Briefly, we classify particles as belonging either to a standard six-membered SP ring or to a *modified* six-membered SP ring. A particle belongs to an SP ring if the number of bonds passed through in moving from one particle of the ring to another is the shortest among all possible paths through the network of bonds. If, in addition, every particle of the ring is also bonded to a single central particle, the particles are said to belong to a modified SP ring. By definition, particles belonging only to SP rings represent regions containing defects, while those belonging to modified SP rings represent ideal crystalline arrangement. Once the positions of the atoms belonging to defect (soliton) locations are obtained, standard cluster counting techniques obtains the coordinates of the atoms associated with each individual defect. We observe that (1) the defects are extended structures consisting of more than one atom and (2) the number of atoms comprising a defect is more or less fixed. We can then easily obtain the center-of-mass coordinates of each defect [i.e., group of pink/light gray particles, see Fig. 2(c)]. In Fig. 2(c), the red and pink colors represent the locally ideal and defective neighborhoods, respectively, inside the two-dimensional strained colloidal crystal showing the stabilization of a soliton lattice at four different temperatures. As T increases, the location and size of the defects become ambiguous due to the presence of random thermal fluctuations.

(2) *The blocking method:* to confirm that the extracted soliton positions are independent of the method used to analyze these configurations, we have an alternate "blocking" method to obtain an independent estimation. Accordingly, we introduce a block length $L_b = n_b a$, where a is the lattice constant of the undeformed lattice. We choose $n_b = 8-12$ and hence L_b such that $n_b \gg 1$ but L_b still clearly less than the typical distance between the solitons. By moving this coarse-graining block along a row in the y direction (in steps of a), we count how many particles n actually fall inside a block. If we work at low enough temperatures, where the mean-square displacement of the particles over the length L_b is still much less than a^2, we obtain $n = n_b$ if no soliton core falls into the block, while we obtain $n = n_b + 1$ if a soliton core falls into the block. Calculating the center of mass of a cluster of adjacent blocks with $n = n_b + 1$ then yields an alternative estimate for the position of a soliton in a system configuration.

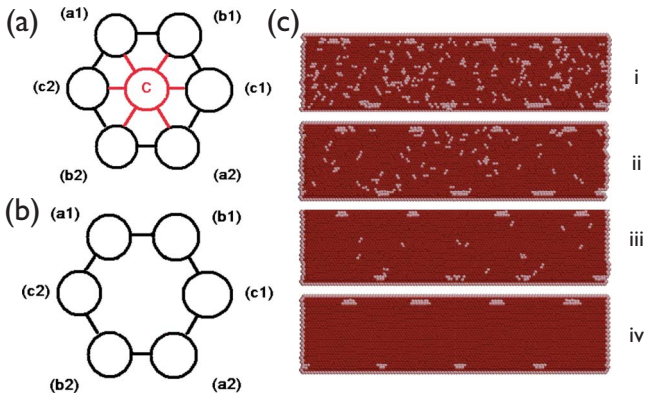

FIG. 2. (Color online) Characterization of the six-membered SP rings: (a) the modified six-membered ring where C is the central particle, (b) an SP-six-membered ring containing three antipodal pairs (a1, a2), (b1, b2), (c1, c2) the shortest paths of equal distance between (a1) and (a2) are through (b1) and (c1) or through (c2) and (b2). (c) The results of two-dimensional ring analysis on 108×30 colloidal crystals. In each case, a lattice consisting of $n_s = 4 = 108/(30-3)$ solitons, comprising two arrays of defects (pink/light gray) near each confining wall, was stabilized at temperatures $T = 0.7(i)$, 0.5(ii), 0.3(iii) and 0.1(iv). Note that as the temperature is increased, random thermal fluctuations produce defects within the bulk of the strip, making the identification of the defects more and more ambiguous.

Both the methods yield the same structure of the soliton lattice. This consists of two identical and strongly coupled one-dimensional arrays of extended defects near each confining wall [Fig. 2(c)]. In Fig. 3(a) we have plotted probability distributions for Δy the distance between the center-of-mass positions y_l, y_{l+1} of neighboring defects $l, l+1$, within each defect array and for Δx the distance between the two arrays. In the inset we have shown a plot of the center-of-mass position y_l of each defect within one array against y_l', the position of the nearest defect in the other. These plots prove that (1) the constituent defect arrays fluctuate mostly parallel to the walls and (2) the fluctuations of the two defect arrays are, as mentioned, strongly coupled resulting in a single effectively one-dimensional lattice of solitons.

Each soliton is then described as an effective point particle of mass M, position y_l and conjugate momentum Π_l. The Hamiltonian for the harmonic chain is given by

$$H_{sol} = \frac{1}{2}\sum_l [\Pi_l^2/M + MC^2(y_{l+1} - y_l - \Delta y_0)^2/(\Delta y_0)^2] \quad (1)$$

where parameter C is the sound velocity and Δy_0 the thermal average of Δy. From Eq. (1) one obtains the correlation function of the mean-square displacements $U_l = y_l - l\Delta y_0$ as [20] $\langle (U_l - U_0)^2 \rangle = l(\Delta y_0)^2 k_B T/(MC^2) = l\delta^2$, the relative displacements Δy_l adding up in a random-walk-like fashion [13].

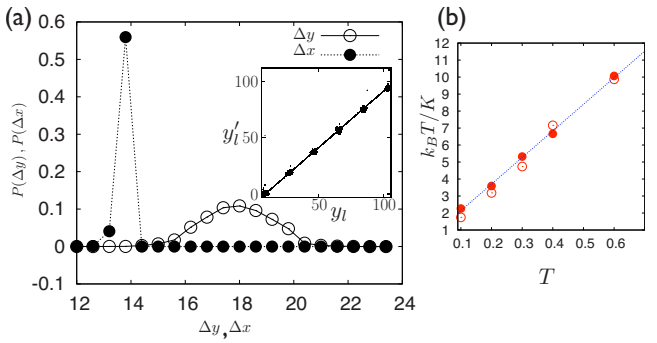

FIG. 3. (Color online) Statistics of defect positions in the soliton lattice. Data for this and subsequent figures are for a system with $L=n_y a$ with $n_y=108$, and $n_s=6$ solitons present after a transition from $n_x=20$ to $n_x=19$. (a) Plot of $P(\Delta y)$ (open circles) and $P(\Delta x)$ (solid circles) at $T=0.2$ for a 108×20 system. Note that $P(\Delta x)$ is an order of magnitude narrower than $P(\Delta y)$. Inset shows a plot of y_l, the position of the l^{th} defect in one array against y_l', the corresponding defect in the other. (b) Plot of k_BT/K, as extracted from $P(\Delta y)$, versus T. Open and closed symbols are the results from the block and the $2d$ ring analysis method, respectively. The straight line is a fit to all data, yielding $K=7.3\pm 0.3$.

As long as $\delta \ll \Delta y_0$, the one-dimensional correlation extends over many solitons, and the term soliton lattice, in a sense, is still meaningful; when δ is no longer much smaller than Δy_0; however, the system rather should be described as a soliton liquid. As is well known, the melting of a one-dimensional crystal is a continuous transition ($\xi \sim 1/T$). If one nevertheless defines [19] an effective melting temperature T_m^{sol} for one-dimensional systems by arbitrarily requiring that their Lindemann parameter $\delta/\Delta y_0 < 0.01$, one would obtain $k_B T_m^{sol}=0.01MC^2$ as the temperature scale that controls the melting of the soliton lattice. Though clearly the melting of the soliton lattice is far from a sharp thermodynamic phase transition, this already suggests that the soliton lattice may melt at rather low temperature, far below the melting temperature $T_m \approx 1.35$ of the bulk two-dimensional crystal at the chosen density [12].

We now compare the probability distribution $P(\Delta y)$ from both the ring analysis method and the blocking method. Figure 4 shows that both methods of analyzing the configurations to identify the solitons agree almost perfectly with each other, and $P(\Delta y)$ is rather well described by a Gaussian, $P(\Delta y)=\sqrt{1/2\pi\delta^2}\exp(-(\Delta y-\Delta y_0)^2/2\delta^2)$ where, for a 108×20 system, we use $\Delta y_0=18=n_y/n_s=108/6$ and the only fit parameter is δ. From Eq. (1) it is obvious that the quantity $K=MC^2/(\Delta y_0)^2=k_BT/\delta^2$ plays the role of an elastic constant. Figure 3(b) therefore plots k_BT/K vs T to test to what extent K is independent of temperature. Note that the resulting value of $K=7.3\pm 0.3$ is about an order of magnitude smaller than typical elastic constants ($\sim 100k_BT/a^2$) of the underlying r^{-12} solid [13], a result which we speculate should hold for similar defect lattices regardless of the nature of the interparticle interactions. Further, for fixed L_y (or n_y), K decreases with increasing n_x (or Δy_0). Finally, we note that the Lindemann ratio 0.01 is reached at an effective melting temperature $T_m^{sol}=0.44$. This value is compatible with the di-

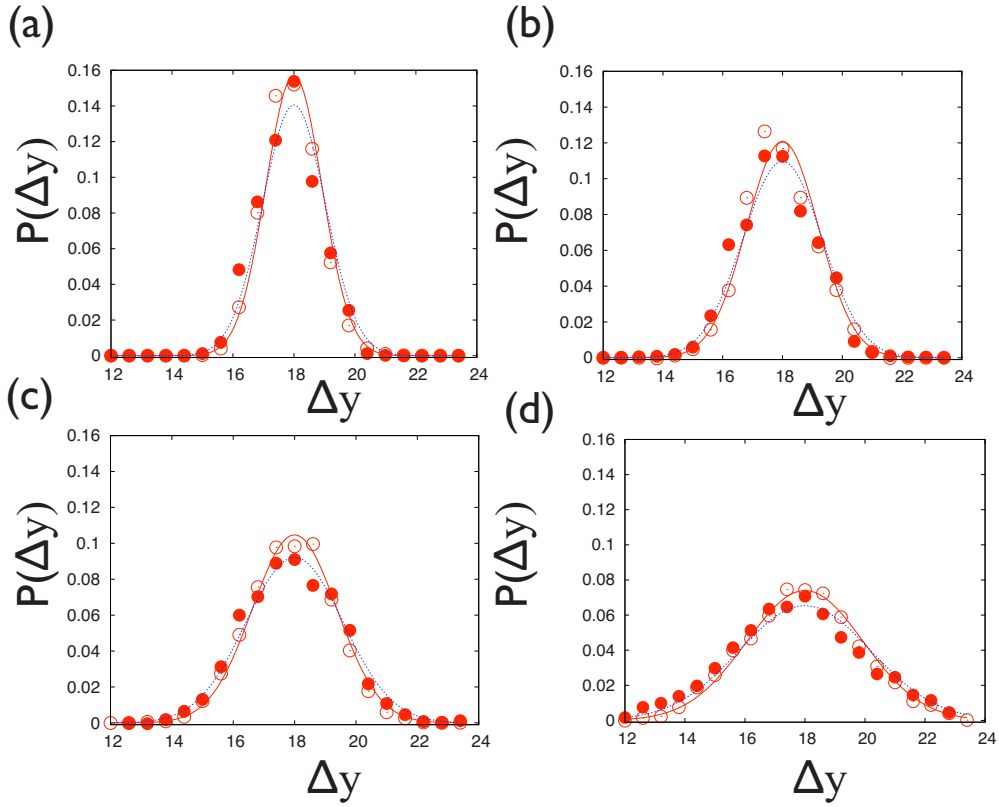

FIG. 4. (Color online) Probability distribution $P(\Delta y)$ versus Δy, for (a) $T=0.1$, (b) 0.2, (c) 0.3, and (d) 0.6. Symbols have the same meaning as in Fig. 3. The lines show the corresponding Gaussian fits.

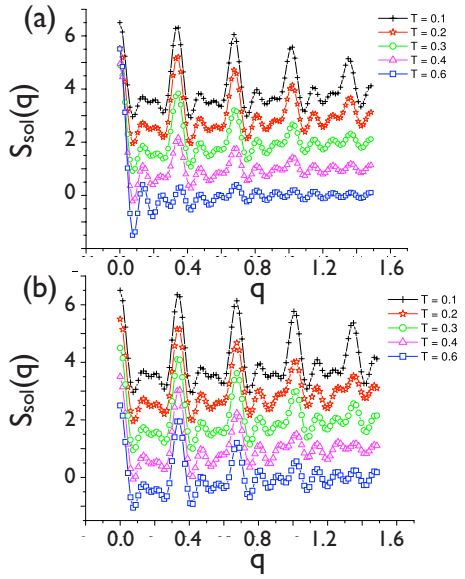

FIG. 5. (Color online) Structure factor of the soliton staircase $S_{sol}(q)$ vs q at temperatures $T=0.1(+)$, $0.2(*)$, 0.3 (○), 0.4 (△), and 0.6 (□). Symbols are the actual simulation data obtained from either the (a) ring analysis or the (b) block analysis; lines are guides to the eyes. Each curve has been shifted by an unit distance in the vertical direction for clarity. Note that both (a) and (b) give comparable results.

rect observation of the effective melting temperature obtained from the structure factor.

Following Ref. [21] one can obtain the structure factor $S_{sol}(q)$ for a finite one-dimensional lattice of n_s soliton, using δ and Δy_0 as parameters,

$$S_{sol}(q) = \frac{1}{2}\sum_{l=1}^{n_s-1} \cos(ql\Delta y_0)\exp\left(-\frac{1}{2}q^2\delta^2 l\right) \qquad (2)$$

While at $T=0$ in the limit L_y and $n_s \to \infty$ the soliton lattice would cause sharp Bragg peaks for all $T>0$ the soliton system is expected to have a liquidlike structure factor. Figure 5 shows simulation data for $S_{sol}(q)$ vs q at various temperatures. We note that at $T=0.1$ indeed the peaks of $S_{sol}(q)$ are already rather sharp, while for $T>0.3$ the structure factor clearly has the character of a fluid. The nature of the curves is well represented by the form given in Eq. (2).

In our previous studies [9], we reported our work on soliton staircases and strain wave patterns in confined soft two-dimensional colloidal crystals. In the present Rapid Communication, we obtain accurate effective interactions between the solitons and report a gradual melting of the soliton superlattice in analogy to that of harmonic chains. We believe that our studies would be useful in designing experimental colloidal systems where such defect lattices in narrow channels may be stabilized. These structures, which have some resemblance to vortex matter in channels [22], may have interesting optical and transport properties. Work along these lines is in progress.

ACKNOWLEDGMENTS

This research was partially supported by the Deutsche Forschungsgemeinschaft, Project No. TR6/C4. Y.-H. C. would like to thank RMIT University, Australia for the hospitality during his academic visits. S.S. thanks DST, Government of India for support.

[1] R. E. Thorne, Phys. Today **49**, 42 (1996).
[2] S. Brown and G. Gruner, Sci. Am. **270**, 50 (1994).
[3] G. Blatter *et al.*, Rev. Mod. Phys. **66**, 1125 (1994).
[4] S. L. Sondhi, A. Karlhede, S. A. Kivelson, and E. H. Rezayi, Phys. Rev. B **47**, 16419 (1993).
[5] F. F. Abraham, W. E. Rudge, D. J. Auerbach, and S. W. Koch, Phys. Rev. Lett. **52**, 445 (1984); J. Villain, in *Ordering in Strongly Fluctuating Condensed Matter Systems*, edited by T. Riste (Plenum, New York, 1980); M. Kardar and A. N. Berker, Phys. Rev. Lett. **48**, 1552 (1982).
[6] P. M. Chaikin and T. C. Lubensky, *Principles of Condensed Matter Physics* (Cambridge University Press, Cambridge, England, 1995).
[7] A. Blaaderen, Prog. Colloid Polym. Sci. **104**, 59 (1997).
[8] K. Zahn and G. Maret, Phys. Rev. Lett. **85**, 3656 (2000); W. Poon, Science **304**, 830 (2004).
[9] Y.-H. Chui, S. Sengupta, and K. Binder, EPL **83**, 58004 (2008); Y.-H. Chui *et al.*, J. Chem. Phys. **132**, 074701 (2010).
[10] G. Piacente, I. V. Schweigert, J. J. Betouras, and F. M. Peeters, Phys. Rev. B **69**, 045324 (2004).
[11] K. Binder, Rep. Prog. Phys. **60**, 487 (1997).
[12] K. Bagchi, H. C. Andersen, and W. Swope, Phys. Rev. E **53**, 3794 (1996).
[13] A. Ricci, P. Nielaba, S. Sengupta, and K. Binder, Phys. Rev. E **75**, 011405 (2007).
[14] D. Chaudhuri and S. Sengupta, Phys. Rev. Lett. **93**, 115702 (2004); J. Chem. Phys. **128**, 194702 (2008).
[15] O. M. Braun and Y. S. Kivshar, *The Frenkel-Kontorova-Model: Concepts, Methods and Applications* (Springer, Berlin, 2004).
[16] M. Koppl, P. Henseler, A. Erbe, P. Nielaba, and P. Leiderer, Phys. Rev. Lett. **97**, 208302 (2006).
[17] B. OMalley, Ph.D. thesis, RMIT University, 2001; B. OMalley and I. K. Snook, Phys. Rev. Lett. **90**, 085702 (2003); J. Chem. Phys. **123**, 054511 (2005).
[18] R. J. Rees, Ph.D. thesis, RMIT University, 2004.
[19] D. S. Franzblau, Phys. Rev. B **44**, 4925 (1991).
[20] V. J. Emery and J. D. Axe, Phys. Rev. Lett. **40**, 1507 (1978).
[21] G. Radons, J. Keller, and T. Geisel, Z. Phys. B: Condens. Matter **50**, 289 (1983).
[22] See N. Kokubo, R. Besseling, and P. H. Kes, Phys. Rev. B **69**, 064504 (2004), and references therein.